Improving performance of A CO2 Thermally Driven Heat Pump Based on a New Optimal High-Pressure Correlation

Ali Salame[1,2,3], Vincent Lemort[2], Pascal Dufour[3], Madiha Nadri[3]

[1]Boostheat Companyz
Lyon, France,

(+33) 0 6 70 84 61, ali.salame@boostheat.com

[2]University of Liège, Energy Systems Research Unit,
Liège, Belgium,
vincent.lemort@uliege.be

[3] Univ Lyon, Université Claude Bernard Lyon 1, CNRS, LAGEPP UMR 5007,
43 boulevard du 11 novembre 1918, F-69100, VILLEURBANNE, France,

pascal.dufour@univ-lyon1.fr

Abstract. Optimizing the performance of CO2 heat pumps often requires an optimal high pressure setpoint, which traditionally depends on the gas cooler outlet temperature and sometimes the evaporation temperature, as proposed in [8]. Despite the variety of correlations available in the literature, no single generalized correlation can be universally applied to all applications. Consequently, it is advisable to determine the optimal correlation specific to each application to achieve the most accurate and relevant results. Boostheat has developed a new thermally driven heat pump with a three-stage thermal compressor to exploit CO2 in its supercritical state. This study, based on a validated model, investigates the impact of various parameters such as the return water temperature, fume and evaporation temperature on the overall coefficient of performance (COP). Using the most significant parameters, we propose a new optimal high-pressure correlation and compare it with the existing ones.

Keywords. CO2, Thermally driven, Heat pumps, Thermal compressor.

Nomenclature

$\dot{m}$	Mass flow rate (G/s)
$\dot{Q}$	Heat capacity (W)
h	Specific enthalpy (J/kg)
Tr	Temperature ratio
p	Pressure (Bar)
Pr	Pressure ratio
T	Temperature (°C)

Special characters

ω_b	Burner fan speed (Rpm)

Subscripts

COP	Coefficient of performance
LHV	Lower heating value
GWP	Global warming potential
TDHP	Thermally driven heat pump
TC	Thermal compressor
CO2	Carbon dioxide
c	Gas cooler
e	Evaporator
t	Total
w	Return water
$comb$	Combustion
rec	Recovery

1 Introduction

Until 1930, CO2 was considered as a widespread refrigerant. Due to the discovery of superior performance artificial refrigerants (CFC and HFC), CO2 was replaced. Forty-four years later, and due to the accumulation of harmful effects done on the ozone layer by these artificial refrigerants, natural refrigerants and specifically CO2 has gained attention again [9], mainly due to its global warming potential (GWP) and ozone depletion layer (ODP) of 1 and 0, respectively. Other advantages include nontoxicity, nonflammability and availability.

In the past decades, CO2 have shown its potential in heat pump applications, as demonstrated in [10, 11, and 17]. Another distinguishable characteristics of CO2 are lower critical temperature of 31.1 °C and high critical pressure of 73.8 bar, which justify why CO2 heat pump cycles are usually designed to operate in the transcritical state, a higher temperature glide. In fact, the effect of the high pressure on the COP seems to be nonmonotonic in the transcritical region, as the high pressure becomes independent from the rejected heat temperature. Among the first attempts to find the optimal high pressure are introducing a graphical method [5] and by comparing different simulated operating conditions [13].

Other research work [2, 6, 8, and 16] obtained high pressure control correlations as a function of gas cooler outlet temperature, and sometimes including also evaporation temperature, as done by the latter two. Their results were based on either simulated models or experimental data on specific range of parameters, proving that gas cooler outlet temperature has greater effect on the COP than evaporation temperature. An optimal high-pressure correlation as function of gas cooler outlet temperature was developed based on experimental data [14], surpassing the performance of correlations in [2 and 6]. No generalized high-pressure correlation for CO2 heat pump, so we believe that each application will have to develop its own correlation, either based on experimental data, or a validated simulated model.

Most of the developed heat pumps today are electrically driven, so little attention was paid to Thermally driven ones, which have its major strength when being powered by waste heat or solar power. Two major types of TDHP applications are absorption and adsorption machines. In this work, we target one specific TDHP application that uses thermally driven compressors previously analyzed [4], which will be called thermal compressor heat pump (TCHP) in this paper. The performance of this heat pump cycle at different operating conditions can be found in [3]. The previous high-pressure correlation used was dependent solely on the return water temperature to the gas cooler and was obtained from trial and error on a real machine. We aim to carry a parametric analysis on a previously validated dynamic model for the gas cooler, where only steady state is simulated. A mass flow rate empirical correlation is derived as function of total pressure ratio, temperature ratio between hot part and cold part of the thermal compressor (TC) as well as the motor speed. By varying the high-pressure value, the COP is simulated at different return water, burner fan seed and evaporation temperature. The optimal COP and high-pressure values are then plotted in a heat pump map for different ranges of these temperatures. After finding the optimal high-pressure correlation again, we compare it with the existing one and Liao's correlation [8]. The Thermophysical properties of CO2 were calculated using CoolProp [1].

2 Thermodynamic model

2.1 Process Overview.

As illustrated in figure 1, the cycle of a TCHP consists of three TCs, three buffers, one gas cooler, one evaporator, internal heat exchanger, flash tanks, two expansion valves and a recovery heat exchanger. At evaporation pressure, CO2 enters the first stage compressor and leaves at a higher pressure. It is then cooled inside buffer 1 with a water flow, and then mixes with the vapor leaving the flash tank in a one-way valve before entering the second TC. The CO2 then leaves at higher intermediary pressure and cooled again inside the second buffer before entering the third TC. At the CO2's highest pressure level and high temperature, CO2 rejects heat into the water entering the gas cooler. It is then cooled again inside an internal heat exchanger by the CO2 leaving the evaporator. After leaving the internal heat exchanger, the CO2 refrigerant is expanded in a high-pressure valve, then enters a flash tank, where the CO2 in its gaseous state is reinjected between the first and second TCs through a one-way valve, and the remaining liquid leaves and expands in a low-pressure valve before finally entering the evaporator. For the water side (heating circuit): smaller part of the water flow goes to the buffers and the TCS, where it is subdivided again between the first two buffers and collected before consequently entering the coolers of the TCs. The larger part of the entering water goes to the gas cooler, where the two parts mix again before entering the recovery heat exchanger, where the resulting fume from the combustion process are cooled.

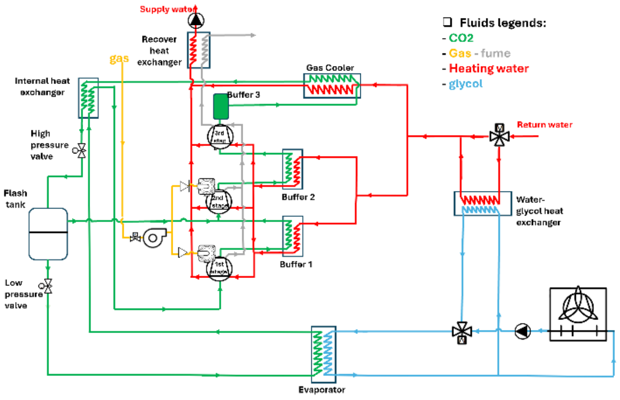

Figure 1: Schematic representation of the TCHP.

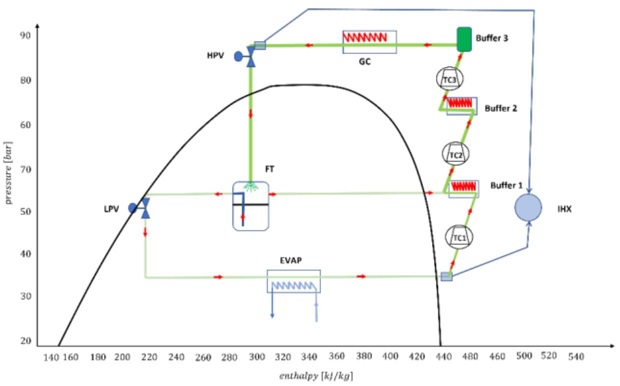

Figure 2: p-h diagram of CO2 in the TCHP cycle.

2.2 COP.

On the gas burning side, the first two TCs are directly heated with burned gas, while the third one is heated with their exhaust gas, before recovering the remaining by water. The heating of the water occurs in several places, in gas cooler which is the main one, that we need to optimize, and the recovered heat in coolers 1,2, and 3 and buffers 1 and 2. Since the

primary source of a TDHP is heat and not electricity, the used COP is a thermal one defined as the released heat energy over the consumed heat. The range of total heating COP as reported in several applications is between 1-1.7 [7]. So, the total COP resulting from the output heat over the input heat can be written as follows:

$$COP_t = \frac{\dot{Q}_c + \dot{Q}_{cooler1,2,3} + \dot{Q}_{buffer1,2} + \dot{Q}_{rec}}{\dot{Q}_{comb}} \quad (1)$$

Where $\dot{Q}_c, \dot{Q}_{cooler1,2,3}, \dot{Q}_{buffer1,2}, \dot{Q}_{rec}$ are the heat recovered from the gas cooler, coolers 1, 2 and 3, the two buffers and the recovery heat exchanger, respectively. $\dot{Q}_{comb}$ is the gas power provided to the cycle. In this heat pump application, optimal performance is defined by maximizing heat rejection in the gas cooler rather than maximizing heat recovery in the other heat exchangers. This being said, the COP term in this work is reduced to be:

$$COP = \frac{\dot{Q}_c}{\dot{Q}_{comb}} \quad (2)$$

Where:

$$\dot{Q}_c = \dot{m}_c\left(h_{c,in} - h_{c,out}\right) \quad (3)$$

Knowing that $h_{c,out}$ is computed from a previously derived and validated dynamic model for the gas cooler. And the combustion power is calculated as function of the methane gas (CH_4) flow rate and the lower heating value (LHV):

$$\dot{Q}_{comb} = \dot{m}_{CH4} LHV \quad (4)$$

2.3 TC Empirical Models.

In this section, we give an insight about the most important component of our cycle which is a TC. In our previous work we have developed simple empirical models for the main thermal compressor performance indicators, such as the mass flow rate and discharge temperature. These models were developed based on collected experimental data from a thermal compressor in a basic single stage heat pump cycle. The derived empirical models in [15] were used to find the TC performance indicators represented in figure 3.

Figure 3 (a) shows that the mass flow rate decreases as pressure ratio increases, while it increases when the speed of motor increases. In the other hand, the discharge temperature increases harmonically with the increase of both motor speed and pressure ratio, as seen in Figure 3 (b). In both plots, a constant temperature ratio is considered: $T_r = 3.2$. It is important to note out that these figures better represent the first two TCs as they are directly heated by gas, while the third TC is heated by the resulting fume from the first two. For this reason and for the sake of simplicity we consider that mass flow rate and the discharge temperature of the third thermal compressor to depend on the total pressure ratio and burner fan speed regulating the amount of gas being burned. The following empirical models are derived from fitting the whole cycle data found in [3] into a polynomial regression type model. The inlet temperature of the gas cooler and the mass flow rate are modeled empirically as follow:

$$\dot{m} = 0.013\omega_b + 13P_{rt} - 0.0044\omega_b P_{rt} - 29.7 \text{ [g/s]} \quad (5)$$

$$T_{c,in} = 0.023\omega_b + 7.4P_{rt} + 0.00076\omega_b P_{rt} + 17 \text{ [°C]} \quad (6)$$

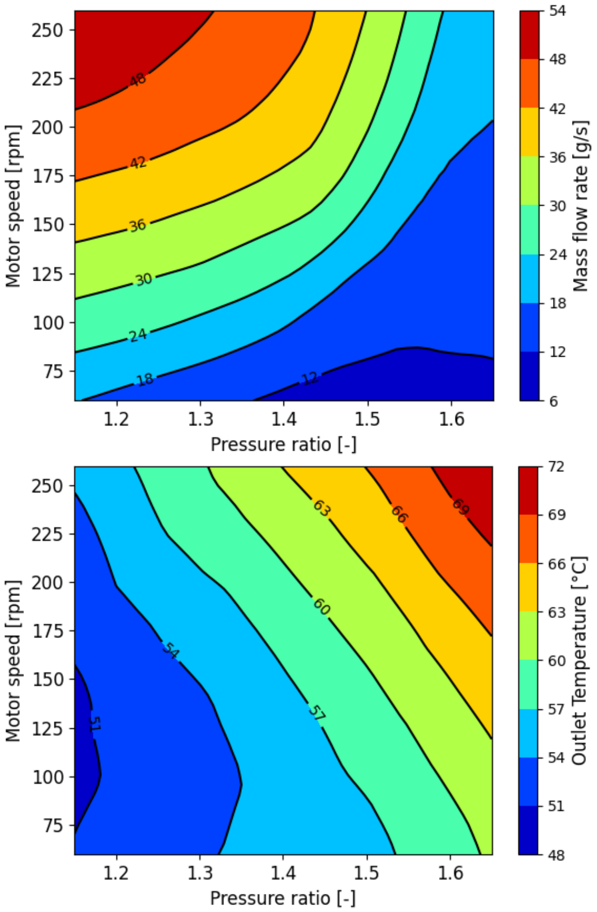

Figure 3: Performance indicators of a single thermal compressor demonstrated by (a) mass flow rate and (b) discharge temperature as function of pressure ratio and motor speed.

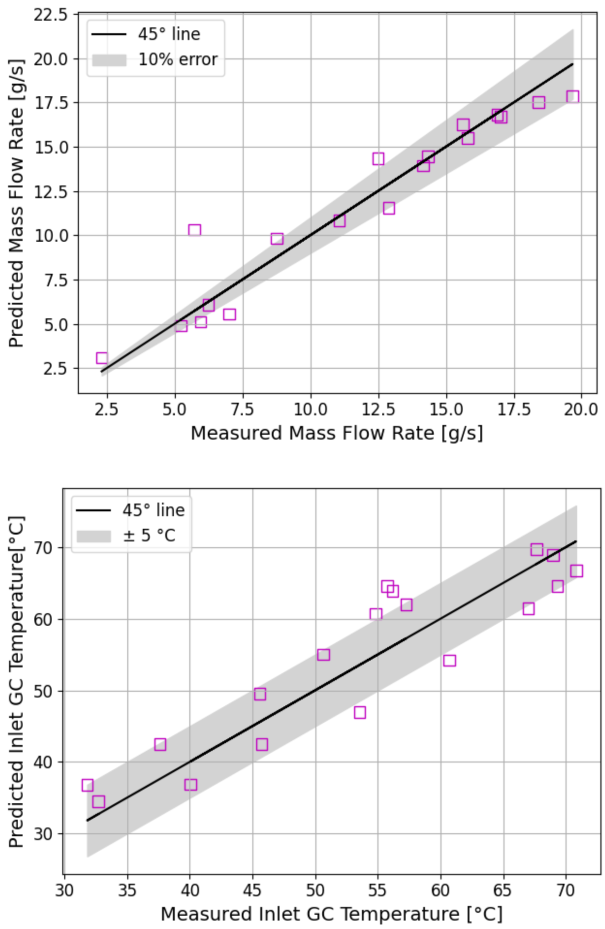

Figure 4: Parity plots between the predicted and measured values of the (a) mass flow rate and (b) inlet temperature of the gas cooler.

Where the total pressure ratio $P_{r_t} = \frac{p_c}{p_e}$, the temperature ratio of the third TC. The combustion power can be presented as function of combustion power:

$$\dot{Q}_{comb} = 1.2\omega_b - 1420.4\,[\mathrm{W}] \qquad (7)$$

Figure 4 demonstrates that the empirical correlations for mass flow rate and gas cooler inlet temperature predict the observed data with a good accuracy, thus reliable for our model-based parameters analysis.

3 Results And Discussions

In this work we consider the return water temperature instead of the gas cooler outlet temperature as it will be more relevant when having two-phase flow at the exit of the gas cooler, which makes it more relevant to consider the return water temperature instead. A parametric study is carried out to show the effect of several parameters on the heating COP. The range of the gas cooler pressure is varied from 58 to 88 bar, the return water temperature (T_w) between 15 and 40 °C, the evaporation temperature (T_e) is varied from -15 °C to 10 °C, and the burner fan speed (ω_b) is between 2000 and 7000 rpm.

3.1 Analysis.

Figures 5, 6, and 7 show the variation of the COP as function of high-pressure values at different evaporation temperatures, with (a) and (b) being top and bottom figures respectively. In figure 5 the return water temperature is fixed at 30 °C and burner fan speed at 4500 rpm. (a) shows that the COP slightly varies as evaporation temperature varies, while (b) shows that at different evaporation temperatures the optimal high-pressure value (characterized by the curve peak) is constant (80 bar). Figure 6 shows the impact of varying the high-pressure and burner fan speed on the COP, while the evaporation temperature is kept constant 0 °C. The figure also shows a slight change in the COP as the burner fan speed varies. Figure 7 shows the impact of varying the return water and high-pressure on the COP. It is seen that varying the return water temperature leads to distinct optimal

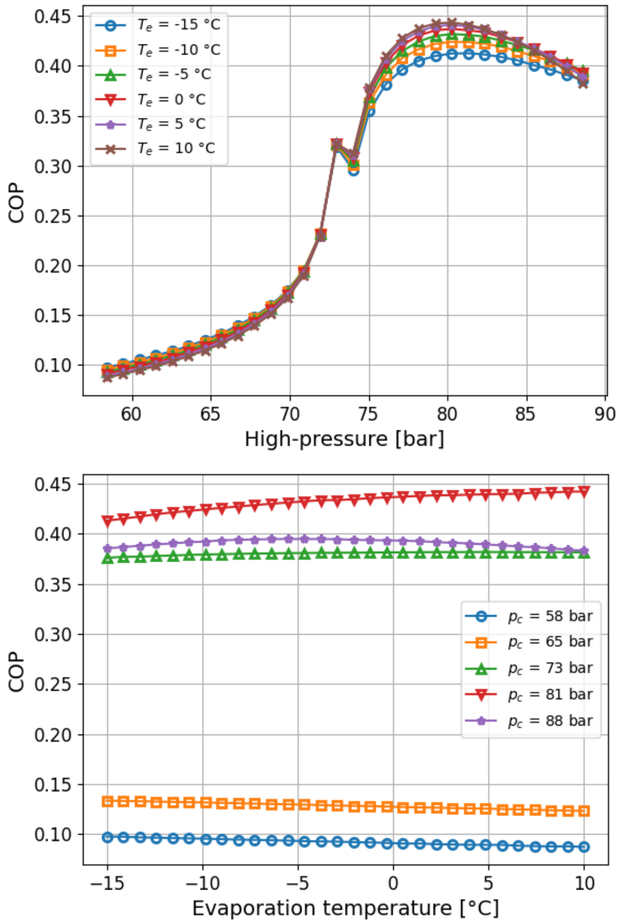

Figure 5: The impact of varying evaporation temperature (high-pressure) on the COP at different high-pressure (evaporation temperature).

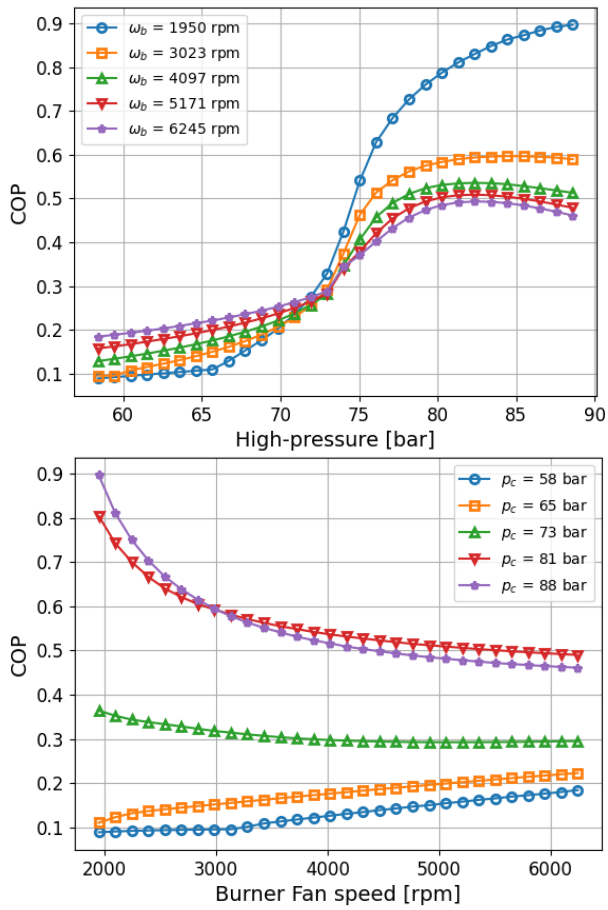

Figure 6: The impact of varying burner fan speed (high-pressure) on the COP at different high-pressure (burner fan speeds).

high-pressure values. As the return water temperature increases (increase of heat load), the COP seems to decrease and the optimal high-pressure increases. It is then concluded that the return water temperature has the highest influence on the COP and the variation of the optimal high-pressure values.

3.2 Optimal High-Pressure.

In this section we aim to find the optimal high-pressure correlation that induces highest COP based on our model, as function of return water temperature which have shown to be the most significant parameter. By simulating the model at different range of return water temperature values, the following optimal high-pressure correlation is obtained:

$$p_{c,new} = 3.3T_w - 0.03T_w^2 + 6.7 \text{ [bar]} \qquad (8)$$

To validate the derived correlation, we apply it on real data and compare it with other correlations.

We use the data from [3], where the TCHP is experimented when the outdoor temperature is between -10 and 12 °C, at water supply temperatures of 55 °C (W55). At each outdoor temperature the machine is automated to deliver the demanded water supply temperature by varying the operating conditions by the TCs. The previous optimal high-pressure correlation was solely and linearly dependent on the return water temperature described as follows:

$$p_{c,old} = 1.47T_w + 31.53 \text{ [bar]} \qquad (9)$$

The derived new correlation, the old one and Liao correlations are compared with the simulated optimal pressure at different outdoor temperatures for W55 in Figure 7. The figure shows the best fit is obtained by the new correlation (absolute average deviation of 2%), followed by 4.5 % deviation by the old one, then Liao's correlation which shows a significant deviation.

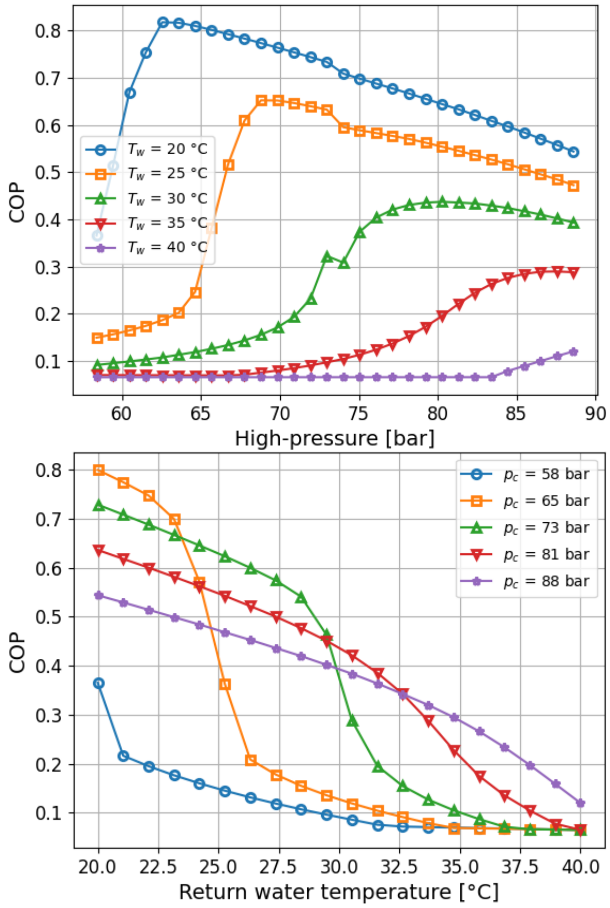

Figure 7: The impact of varying return water temperature (high-pressure) on the COP at different high-pressure (return water temperature).

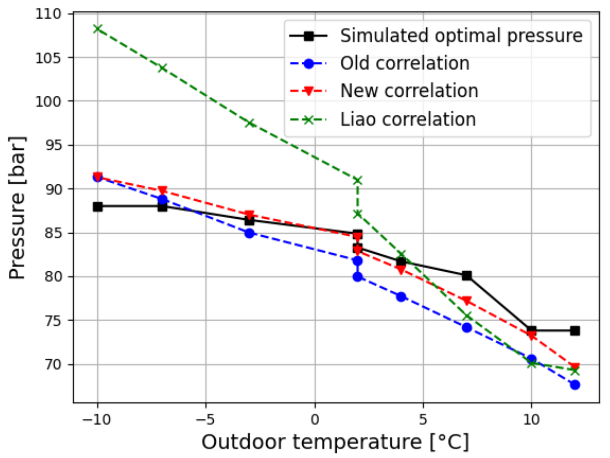

Figure 8: Comparison between different optimal high-pressure correlations with the simulated one.

4 Conclusion

Although TDHPs are not as attractive as electrically driven heat pumps, it remains interesting when it comes to valorising waste heat. As a conventional CO2 heat pump, the high-pressure plays a crucial role in obtaining the optimal COP. We studied the effect of varying the evaporation, burner fan speed, and return water temperatures on the COP, which showed the former two parameters have a neglected effect compared to the latter one. Therefore, based on carried simulations, we derived an optimal high-pressure correlation as function of return water temperature and compare it with other existing correlations. This correlation can be imposed as an optimal high-pressure setpoint for future control and optimization attempts.

Acknowledgement

The French ministry of higher education and research is acknowledged for the financial support of this CIFRE PhD thesis 2022-0549.

References

[1] Bell, I.H., Wronski, J., Quoilin, S., Lemort, V., 2014, Pure and Pseudo-pure Fluid Thermophysical Property Evaluation and the Open-Source Thermophysical Property Library CoolProp, *Ind. Eng. Chem. Res.*, 53(6), p. 2498-2508.

[2] Chen, Y., & Gu, J. (2005). The optimum high pressure for CO2 transcritical refrigeration systems with internal heat exchangers. International Journal of Refrigeration, 28, 1238-1249.

[3] H. Fallahsohi, Energy analysis of the heat pump operating with supercritical CO2 driven by thermal compression. American Journal of Engineering Research (AJER), Volume-12, Issue-11, pp: 61-74, 2023.

[4] R. Ibsaine et al., Modelling of a new thermal compressor for supercritical CO2 heat pump, *Energy*, Volume 117, Part 2, p. 530-539.

[5] H. Inokuty, Graphical method of ending compression pressure of CO2 refrigerating machine for maximum coefficient of performance, in: Proceedings of the 5th International Congress Refrigeration, Rome, pp. 185-192, 1928.

[6] F. Kauf Determination of the optimum high pressure for transcritical CO2-refrigeration cycles. International Journal of Thermal Sciences, 38, 325-330, 1999.

[7] A. Kühn, Thermally Driven Heat Pumps for Heating and Cooling, 2013.

[8] S. M. Liao et al., A correlation of optimal heat rejection pressures in transcritical carbon dioxide cycles. Applied Thermal Engineering, 20, 831-841, 2000.

[9] G. Lorentzen, Revival of carbon dioxide as a refrigerant. International Journal of Refrigeration, 17, 292-301, 1994.

[10] P. Neksa, CO2 heat pump systems, Int J Refrig 25, p. 421–427, 2002.

[11] P. Neksa et al., CO2-heat pump water heater: characteristics, system design and experimental results, Int J Refrig 21 (3), p. 172–179, 1998.

[12] A. Okasha and N. Müller. Simulation and Performance Correlation for Transcritical CO2 Heat Pump Cycle, 2018.

[13] J. Pettersen and G. Skaugen, Operation of trans-critical CO2 vapour compression circuits in vehicle air conditioning, in: Proceedings of the New Applications of Natural Working Fluids in Refrigeration and Air Conditioning, Hannover, Germany, pp. 495-505, 1994.

[14] P. C. Qi et al., Experimental investigation of the optimal heat rejection pressure for a transcritical CO2 heat pump water heater, Applied Thermal Engineering, 56, 120-125, 2013.

[15] A. Salame et al., An Empirical Model for a CO2 Thermal Compressor Based on Experimental Data. International Compressor Engineering Conference. Paper 2868., 2024.

[16] J. Sarkar et al., Optimization of a transcritical CO2 heat pump cycle for simultaneous cooling and heating applications. International Journal of Refrigeration, 27, 830-838, 2004.

[17] M. G. Yarral et al., Performance of a transcritical CO2 heat pump for simultaneous refrigeration and water heating. In: XX Int. Congress of Refrigeration, Sydney, Paper 651, 1999.